HHS Public Access

Author manuscript

Virology. Author manuscript; available in PMC 2016 July 01.

Published in final edited form as:

Virology. 2015 July ; 481: 199–209. doi:10.1016/j.virol.2015.02.043.

DECAPPING PROTEIN 1 PHOSPHORYLATION MODULATES IL-8 EXPRESSION DURING RESPIRATORY SYNCYTIAL VIRUS INFECTION

Laura L. Dickey[a,b], **Julie K. Duncan**[a,c], **Timothy M. Hanley**[a,b], and **Rachel Fearns**[a]

Laura L. Dickey: laura.dickey@path.utah.edu; Julie K. Duncan: jkdrz3@health.missouri.edu; Timothy M. Hanley: timothy.hanley@hsc.utah.edu

[a]Department of Microbiology, Boston University School of Medicine, 72 E. Concord St., Boston, MA 02118, USA

Abstract

Respiratory syncytial virus (RSV) is a negative-strand RNA virus that is an important cause of bronchiolitis and pneumonia. We investigated the effect of RSV infection on the expression patterns of cellular proteins involved in regulating mRNA translation and degradation, and found that a processing-body protein involved in mRNA degradation, decapping protein 1a (DCP1), was phosphorylated rapidly following infection. UV-inactivated and sucrose-purified RSV were sufficient to mediate DCP1 phosphorylation, indicating that it occurs as a consequence of an early event in RSV infection. Analysis using kinase inhibitors showed that RSV-induced DCP1 phosphorylation occurred through the ERK1/2 pathway. The DCP1 phosphorylation sites were limited to serine 315, serine 319, and threonine 321. Overexpression of wt DCP1 led to a decrease in RSV-induced IL-8 production, but this effect was abrogated in cells overexpressing phosphorylation-deficient DCP1 mutants. These results suggest that DCP1 phosphorylation modulates the host chemokine response to RSV infection.

Keywords

decapping protein 1a; DCP1a; respiratory syncytial virus; IL-8; processing bodies; stress granules

INTRODUCTION

RSV is one of the leading causes of pneumonia-related deaths in infants, the elderly, and immunocompromised persons worldwide. It is estimated that between 75,000 and 125,000

Corresponding author: Rachel Fearns, rfearns@bu.edu, 617-638-4034, Boston University School of Medicine, Department of Microbiology L501, 72 E. Concord St., Boston, MA 02118.

[b]Present address: Department of Pathology, University of Utah School of Medicine, 15 N. Medical Dr., Salt Lake City, UT 84112, USA;

[c]Present address: University of Missouri School of Medicine, One Hospital Drive, MA204, DC018, Columbia, MO, USA

infants in the United States are hospitalized annually with RSV infection, accounting for approximately 25% of pediatric pneumonia and up to 70% of pediatric bronchiolitis hospitalizations (1). The global burden of RSV is approximately 64 million cases and 160,000 deaths per year (2). Unfortunately, there are currently neither vaccines nor effective treatments for the virus.

Immune responses to RSV are characterized by significant inflammation that can contribute to disease pathogenesis, particularly when bronchioles and airways become clogged with cells, debris, and fluids. RSV infection induces the secretion of several chemokines, including RANTES, MIP-1α, MIP-1β, IL-8, and fractalkine (3), which recruit large numbers of immune cells to the sites of infection. IL-8 recruits neutrophils, which are the dominant cells found in the bronchial lavage and nasopharyngeal secretions of infants hospitalized for RSV disease (4). Neutrophils are important for RSV clearance, but they also cause significant cell damage (5, 6), and granulocytes recruited to airways can directly mediate the destruction of infected cells (6).

RSV is a negative-sense RNA virus in the family *Paramyxoviridae*. RSV enters host cells via macropinocytosis and acid-independent membrane fusion (7). The viral nucleocapsid, consisting of viral RNA encapsidated with nucleoprotein (N) and associated with polymerase proteins, is released into the cytoplasm where the viral RNA-dependent, RNA polymerase performs both transcription to produce viral mRNAs and replication to generate antigenome and genome (8). The production of new genomes results in the formation of large cytoplasmic inclusion bodies containing viral nucleocapsids (9, 10). At later stages in the infection cycle, nucleocapsids are transported to the plasma membrane where they assemble with other viral proteins and are released by budding (8).

A number of studies have demonstrated relationships between viruses and various cellular proteins and granular structures involved in mRNA processing (11–14). A significant portion of this work has focused on two inter-related cytoplasmic ribonucleoprotein granules: stress granules and processing bodies (P-bodies). Stress granules are rapidly induced in response to cellular stress and are comprised of stalled translation-initiation complexes that correlate with translational shut-off (15). These granules are believed to be involved in mRNA triage and storage during stress conditions (15). We have previously shown that RSV suppresses stress-granule formation (16). It has also been shown that efficient RSV replication depends on a stress granule protein, G3BP (17), so it is possible that repressing stress granule formation might aid RSV replication both by enabling efficient viral protein expression and maintaining free G3BP. The mechanism by which RSV represses stress granule formation is unknown, but appears to involve a non-translated promoter region in the RSV genome called the trailer (16), as well as inhibition of PKR activity by the viral N protein (18). P-bodies are cytoplasmic granules believed to be involved in nonsense-mediated mRNA decay and the microRNA gene-silencing pathway (19). They are constitutively present in the cytoplasm of most cells; however, their distribution can become altered during stress conditions (20, 21). P-bodies contain proteins involved in the 5′ – 3′ mRNA degradation pathway, including decapping protein 1 (DCP1), a requisite mRNA-decapping cofactor (22).

Initially, we set out to investigate the effect of RSV infection on the expression levels of stress-granule and P-body proteins as a means to help determine the mechanism by which stress-granule formation is inhibited. Most of the proteins we examined showed no change in expression following RSV infection and did not provide insight into stress granule inhibition. However, we found that exposure of cells to RSV resulted in rapid phosphorylation of DCP1. A relationship between RSV and DCP1 has not been previously characterized. Here we describe the process by which DCP1 becomes phosphorylated and show that this modification tampers the IL-8 response to RSV infection.

RESULTS

RSV infection resulted in the phosphorylation of DCP1

In a previous study we showed that RSV is able to interfere with the formation of stress granules (16), indicating that there is an interaction between RSV and cellular RNA pathways involved in RNA stability. To follow up on this finding, we investigated whether RSV has a detectable effect on the abundance of proteins involved in post-transcriptional control. HEp-2 cells were mock infected or infected with increasing doses of RSV. Eighteen hours after infection, cell lysates were harvested and analyzed using Western blot analysis with antibodies toward a selection of stress granule and P-body-associated proteins. As a comparison, cells were treated with arsenite, an inducer of oxidative stress, for 30 minutes prior to harvest and analysis. As shown in Figure 1A, neither the levels nor migration patterns of DCP2, EDC3, EDC4, eIF3, Xrn1, TIAR, TIA-1, eIF3, or G3BP were altered either following infection with RSV or arsenite treatment. In contrast, the electrophoretic mobility and abundance of DCP1 was altered in RSV-infected cells. In mock-infected cells, DCP1 migrated as a doublet (Figure 1A, top panel, lane 1); however, in arsenite-treated cells (lane 2) or cells infected with RSV at an moi of 1 or 5 (lanes 5 and 6, respectively), DCP1 migrated as only the upper band (the migration shift can also been seen more clearly in panel C). In addition, the abundance of DCP1 was increased in these cells. These results indicate that RSV has a dose-dependent effect on DCP1 expression and modification. To determine whether RSV infection results in an altered DCP1 migration pattern and abundance in another cell type, we analyzed DCP1 expression in RSV infected A549 cells and obtained similar results, demonstrating that this was not a cell specific phenomenon (Figure 1B). In all the following experiments we used HEp-2 cells (an epithelial cell line that supports efficient RSV replication). The reason for this is that we were able to achieve higher transfection efficiency in HEp-2 than in A549 cells, which was essential for subsequent experiments in this study.

A number of studies have shown that a variety of cellular changes, including arsenite-induced oxidative stress, can cause DCP1 to become phosphorylated. To determine if the change in DCP1 migration observed during RSV infection was due to phosphorylation, we assessed whether DCP1 migration was altered by phosphatase treatment. HEp-2 cells were mock infected, treated with sodium arsenite (as a positive control for DCP1 phosphorylation), or infected with RSV. Cell lysates were then either mock treated or treated with λ-phosphatase, which dephosphorylates serine, threonine, and tyrosine residues. Samples were analyzed by Western blotting with a DCP1 specific antibody (Figure 1C).

Cell lysates that were mock treated with phosphatase showed a similar DCP1 migration pattern as in Figure 1A and B: DCP1 from mock-infected cells migrated as a doublet (Figure 1C, lane1), while DCP1 from arsenite-treated and RSV-infected cells migrated as only the upper band (Figure 1C, lanes 3 and 5). In contrast, the samples from each group that were treated with phosphatase migrated slightly more rapidly than the lower band from mock-infected cells (Figure 1C, lanes 2, 4, and 6). These results show that DCP1 is present in both hypo- and hyperphosphorylated forms in mock infected HEp-2 cells and that in response to RSV, the hyperphosphorylated form (upper band) is dominant. Thus, RSV infection results in the phosphorylation of DCP1.

DCP1 was phosphorylated early in response to exposure to RSV, but independently of viral replication

The virus stock that was used to perform the experiments shown in Figure 1 consisted of clarified supernatant from RSV-infected cells. The cytokine IL-1α has been shown to induce DCP1 phosphorylation (21), raising the possibility that a soluble factor released from the cells used to generate the virus stock could be responsible for inducing DCP1 phosphorylation, rather than RSV *per se*. Therefore, we compared the effect of exposing cells to unpurified RSV versus RSV that had been purified onto a sucrose cushion. In both cases, a time course was performed to examine the kinetics of DCP1 phosphorylation. HEp-2 cells were exposed to RSV for varying lengths of time, from 15 minutes to 24 h. Cell lysates were harvested, and DCP1 was examined by Western blot analysis. DCP1 was phosphorylated within 15 minutes of exposure to RSV, and remained phosphorylated throughout infection with both unpurified and sucrose-purified RSV (Figure 2A, top two panels). Because stressors, including osmotic stress, have been shown to affect DCP1 phosphorylation (21), a control was performed to confirm that the sucrose that would be present in sucrose-purified RSV had no effect. To accomplish this, sucrose was added to cell culture medium at an equivalent concentration as in the sucrose-purified RSV. This treatment had no detectable effect on DCP1 phosphorylation (data not shown). These results suggest that DCP1 phosphorylation was triggered by an early event in RSV infection, and that RSV alone was sufficient to mediate the effect, independently of soluble factors that might have been present in the virus inoculum. To determine whether RSV replication is necessary for DCP1 phosphorylation, the time course described above was also performed with UV-inactivated unpurified or sucrose-purified RSV (Figure 2A, lower two panels). Cells treated with UV-inactivated RSV showed a transient increase in DCP1 phosphorylation, corresponding with the time frame that virus was in contact with cells (Figure 2A, lower two panels, lanes 2–4). Once the media was replaced, the band of hypophosphoryated DCP1 reappeared (Figure 2A, lower two panels, lanes 5–7); however, the upper band remained dominant, distinguishing cells exposed to RSV from mock-infected cells (compare lanes 1 and 7). These results indicate that DCP1 may become phosphorylated independently of RSV replication, but that RSV replication was necessary to maintain DCP1 in a near-completely hyperphosphorylated state throughout infection.

Cytokines released from RSV-infected cells also caused phosphorylation of DCP1

Although the experiment shown in Figure 2A demonstrated that RSV alone was sufficient to cause DCP1 phosphorylation, these results did not exclude the possibility that factors

secreted by infected cells could also have an effect. To determine whether factors in the supernatant (other than RSV) were able to induce DCP1 phosphorylation, the supernatant from RSV-infected cells was subjected to ultra-high velocity centrifugation to pellet the virus. The supernatant fraction was collected and was found to have minimal residual virus (80 and 150 pfu/ml, in two independent experiments). HEp-2 cells were mock treated, treated with supernatant from RSV-infected cells, or incubated with purified RSV as a control. At 1 h post treatment or infection, cells were either harvested directly, or the medium was replaced and the cells were harvested at 18 h post treatment, and the samples were analyzed as described above. Analysis of cell lysates collected at 1 h post treatment showed that while DCP1 from mock-infected cells migrated as a doublet, DCP1 from cells treated with supernatant migrated primarily as the upper band, similarly to DCP1 from cells infected with RSV (Figure 2B, upper panel). In contrast, in samples collected at 18 h post treatment, DCP1 in supernatant-treated cells migrated as a doublet, similarly to mock infected cells (Figure 2B, lower panel). These results indicate that one or more soluble factors released into the supernatant of RSV-infected cells was able to mediate DCP1 phosphorylation; however, the effect was transient, in contrast to RSV infection-mediated DCP1 phosphorylation.

RSV infection of epithelial cells *in vitro* results in induction of a large number of cytokines, which could be the soluble factors responsible for stimulating DCP1 phosphorylation in the experiment shown in Figure 2B (upper panel). To test this possibility, we examined the effects of three cytokines shown previously to be released by RSV infected epithelial cells cultured *in vitro*: IL-1β, TNF-α (23), and IFN-α (24, 25). Cells were treated with varying concentrations of IL-1β, TNF-α, or IFN-α for one hour, then lysed and assessed for DCP1 phosphorylation. As shown in Figure 2C, DCP1 was phosphorylated in response to all tested concentrations of IL-1β and TNF-α. In contrast, treatment with IFN-α did not result in DCP1 phosphorylation at any of the concentrations tested. This result shows that some, but not all, cytokines can stimulate DCP1 phosphorylation. Together with the data presented in Figure 2A, these results indicate that RSV infection results in DCP1 phosphorylation through two paths: first through a direct response of the cell to virus exposure, and second as a response of the cell to some of the cytokines released as a consequence of RSV infection.

RSV infection resulted in decreased localization of DCP1 to P-bodies

Others have shown that DCP1 phosphorylation correlates with changes in P-body distribution and number. However, these effects appear to be highly complex, with different inducers of DCP1 phosphorylation resulting in widely different outcomes (20, 21). Therefore, we assessed whether RSV infection altered the subcellular location of DCP1. HEp-2 cells were mock infected or infected with RSV. At various times post infection, cells were fixed and examined using immunofluorescence (Figure 3). DCP1 in mock-infected cells appeared in numerous small, cytoplasmic puncta, characteristic of P-bodies, with an average of 15.5 +/− 1.22 SEM DCP1-containing puncta per cell. The number of DCP1-containing cells infected with RSV was similar to DCP1 from mock-infected cells early during infection; however, later in infection the number of DCP1-containing puncta was significantly decreased, with means of 8.6 +/− 0.97 and 6.8 +/− 0.96 puncta per cell at 12 and 24 h post infection, respectively. These results suggest that RSV infection may alter

DCP1 inclusion in P-bodies late in infection; however there was no obvious correlation between the change in the phosphorylation status of DCP1 and P-body distribution or number.

DCP1 was phosphorylated by the ERK1/2 pathway following exposure of cells to RSV

Having found that DCP1 was phosphorylated rapidly following exposure of cells to RSV, we sought to determine which kinase pathway was responsible. Previous studies have demonstrated JNK (21) and/or ERK2 (26) pathway involvement in DCP1 phosphorylation under various conditions. Both JNK and ERK1/2 are mitogen-activate protein kinases (MAPKs) that become activated in response to stress. To examine whether known MAPK pathways were responsible for RSV-mediated DCP1 phosphorylation, we assessed whether MAPK activation correlated temporally with DCP1 phosphorylation during RSV infection. HEp-2 cells were mock infected or infected with sucrose-purified RSV. Cells were harvested at a range of time points from 5 minutes to 24 h post infection, and ERK1/2, JNK, p38 and ERK 5 activation were assessed using Western blot analysis with antibodies specific to total or phosphorylated MAPK proteins. Phosphorylation of DCP1 was also assessed as described above. As a control, uninfected cells were treated with arsenite for 30 minutes prior to harvest. As shown in Figure 4A, all MAPKs were activated in response to arsenite, confirming the sensitivity of the phosphoprotein-specific antibodies. In contrast, the MAPKs were differentially activated in response to RSV. Increased ERK1/2 activation occurred within 5 minutes of RSV infection and ERK1/2 remained activated throughout infection, consistent with previously published data (26). The extent of ERK1/2 activation during RSV infection was greater than observed following arsenite treatment. A low level of p38 phosphorylation was detectable at 5 and 15 minutes post infection, but returned to baseline activation thereafter. JNK and ERK5 did not show significant levels of phosphorylation during infection. These results identified ERK1/2 as the most likely MAPK responsible for RSV-mediated DCP1 phosphorylation.

To confirm if ERK1/2 was responsible for RSV-mediated DCP1 phosphorylation, we examined the effect of treating cells with a panel of pharmacological MAPK inhibitors (Figure 4B). 5Z-7-oxozeanol has been demonstrated to strongly inhibit MKKK TAK1, and thereby repress ERK1/2, JNK, and p38 activation (27–29). Both U0126 and PD98059 inhibit both MEK1 and MEK5, and thereby inhibit activation of ERK1/2 and ERK5 (30). PD184352 inhibits both ERK1/2 and ERK5 at 20 μM, but only ERK1/2 at 2 μM (30). SB203580 specifically inhibits p38 activation (30). SP600125 is relatively non-specific, but strongly inhibits JNK activation (30, 31). HEp-2 cells were mock treated with DMSO or treated with the indicated inhibitor. One hour after treatment, cells were mock infected or infected with RSV in the presence of the inhibitors. One hour post infection, cells were lysed and DCP1, phosphorylated ERK1/2, and total ERK1/2 were assessed by Western blot analysis. This analysis showed that RSV-induced ERK1/2 activation was blocked by 5Z-7-oxozeanol, U0126, and PD184352, as expected (Figure 4C, top panel, compare lane 3 with lanes 4, 5, 7, and 8). In contrast, treatment of cells with SB203580 and SP600125 did not inhibit ERK1/2 activation, and treatment with PD98059 had an intermediate effect (Figure 4C, top panel, lanes 9, 10 and 6, respectively). Examination of DCP1 showed that treatment of RSV infected cells with inhibitors that reduced activation of ERK1/2 resulted in DCP1

migrating as a doublet, similarly to mock infected cells (Figure 4C, third panel, compare lane 1 with lanes 4–8, panel 4D). This indicates that the ERK1/2 pathway is responsible for DCP1 phosphorylation during RSV infection. In contrast, DCP1 from RSV-infected cells pretreated with SP600125 (Figure 4C, third panel, lane 8) or SB203580 (Figure 4C, third panel, lane 7) migrated as the upper phosphorylated band, indicating that neither JNK nor p38 was involved in RSV-mediated DCP1 phosphorylation (Figure 4D). These results confirm that DCP1 phosphorylation is modulated by MAPK pathways and demonstrate that activation of the ERK1/2 pathway is required for DCP1 to become phosphorylated following cell exposure to RSV.

DCP1 was phosphorylated at S315, S319 and T321 during RSV infection

Other studies have identified three potential phosphorylation sites on DCP1: S315, S319 and T321 (20, 21, 32). To investigate whether these sites were phosphorylated in response to RSV infection, expression plasmids were generated that contained DDK-tagged DCP1 in which S315, S319, and T321 of DCP1 were each individually substituted, or all substituted (to generate a triple mutant), with alanine. HEp-2 cells were transiently transfected with each of the plasmids and subsequently infected with RSV for 24 h. DCP1 phosphorylation and RSV protein expression were assessed by Western blot analysis. The different forms of DCP1 were somewhat difficult to discern using the anti-DCP1 antibody because this antibody detected both the hypo- and hyperphosphorylated forms of both endogenous and plasmid-expressed DCP1, which all migrated close to one another; however, this analysis showed that DDK-DCP1 was efficiently expressed compared to endogenous DCP1 (Figure 5A, upper panel, e.g. compare lane 1 with 3, and 2 with 4). Analysis with an anti-DDK antibody allowed the effects of the substitutions on DCP1 phosphorylation to be determined (Figure 5A, lower panel). Overexpressed wt DDK-DCP1 showed a similar pattern of phosphorylation as endogenous DCP1 with DDK-DCP1 migrating as a doublet in lysates from mock-infected cells, and as a dominant upper band in lysates from RSV-infected cells. In contrast, S315A DDK-DCP1 had a different migration pattern in RSV infected cells, with the upper band migrating more rapidly than that of wt DDK-DCP1, indicating decreased phosphorylation. The migration patterns of the cells overexpressing the DCP1 variants S319A or T321A were also slightly altered compared to wt DDK-DCP1, indicating decreased phosphorylation. In each case, the lower band was more prominent compared to wt transfected, RSV infected samples, but not as prominent as in mock-infected cells. These findings suggest that S315, S319 and T321 all contributed, to various degrees, to RSV-mediated DCP1 phosphorylation. The triple-DCP1 mutant migrated as only the lower band of the doublet, both in mock and RSV infected cells, confirming that the detectable change in wt DCP1 phosphorylation was entirely due to phosphorylation of S315, S319 and T321. Collectively, these results demonstrate that RSV-mediated phosphorylation is limited to residues S315, S319 and T321 of DCP1.

DCP1 phosphorylation affected RSV-induced IL-8 production

The ability to overexpress phosphorylation-deficient DCP1 allowed us to explore the significance of DCP1 phosphorylation during RSV infection. DCP1 phosphorylation has been shown to enhance its interaction with the decapping enzyme DCP2, which could affect mRNA decapping and stability (26). Furthermore, DCP1 phosphorylation has been shown to

affect the levels of certain chemokines produced by cells, in particular IL-8 (21). IL-8 is a key chemokine released in response to RSV infection and can be expressed by epithelial cells. Therefore, we examined the effect that DCP1 overexpression and phosphorylation had on RSV protein expression and IL-8 production. HEp-2 cells were mock transfected with empty vector or transfected with a plasmid expressing GFP, as negative controls, or transfected with wt or mutant DDK-DCP1. At 24 h post transfection, cells were infected with RSV at moi of 5. Supernatants were collected at 0, 2, 8 and 24 h post infection and cell lysates were collected at 0 and 24 h post infection. Western blot analysis of the cell lysates using a DCP1 specific antibody confirmed that DDK-DCP1 was significantly overexpressed compared to wt DCP1 (Figure 5B, compare lanes 1, 2 and 7). Analysis using a polyclonal anti-RSV antibody (Figure 5B) and quantification (not shown) showed that overexpression of wt or mutant DCP1 did not significantly affect RSV protein expression, indicating that DCP1 does not affect RSV gene expression or viral replication over a single growth cycle. ELISA determination of IL-8 protein levels in the supernatant showed that at 0 and 2 hpi there were only background levels of released IL-8 protein (not shown). However, the levels of secreted IL-8 increased by 8 hours post infection, and amplified significantly (more than 20-fold) between 8 and 24 h post infection. Overexpression of the DCP1 mutants had no detectable effect on the kinetics of the IL-8 response, but did have a statistically significant effect on its magnitude. Overexpression of wt DCP1, which was present in both a hypo- and hyperphosphorylated form, resulted in a greater than two-fold decrease in IL-8 levels at 24 h post infection. This decrease was almost completely abrogated by the triple-A mutation, which is completely DCP1 phosphorylation deficient (Figure 5C). These results demonstrate that in the context of RSV infection, IL-8 protein expression may be inhibited by hyperphosphorylated DCP1, indicating a potential role for DCP1 phosphorylation in chemokine regulation.

DISCUSSION

In this study we have presented novel findings characterizing the relationship between RSV and DCP1, a cellular protein involved in decapping specific subsets of mRNAs in order to regulate their expression. We demonstrated that RSV infection leads to both the phosphorylation of DCP1 via the ERK1/2 pathway, as well as increased DCP1 expression. Both these effects combine to modulate expression of IL-8.

While DCP1 phosphorylation has been described previously, this is the first time it has been shown to occur in response to viral infection. As shown in Figure 2A, DCP1 became phosphorylated within 15 minutes of exposure of cells to RSV and remained in phosphorylated form throughout the course of infection. This rapid modification early in infection suggested that DCP1 phosphorylation occurs independently of virus gene expression, and this was confirmed in experiments using UV-inactivated RSV. In addition, we demonstrated that sucrose-purified RSV stimulated DCP1 phosphorylation to a similar extent as unpurified virus. Together, these findings show that DCP1 phosphorylation occurs in response to an early event in the RSV replication cycle, such as attachment, fusion, or cell entry. Although purified RSV was sufficient to stimulate DCP1 phosphorylation, we showed that one or more soluble factors might also contribute to the effect. Exposure of cells to UV-inactivated RSV resulted in only transient phosphorylation of DCP1, indicating that viral

replication was important for sustaining the response, and we found that the supernatants of RSV-infected cells (from which almost all infectious virus was removed) were able to mediate transient DCP1 phosphorylation (Figure 2B). These findings suggest that although the virus *per se* can cause DCP1 phosphorylation, factors secreted as a consequence of RSV replication may contribute to sustained DCP1 phosphorylation during infection. Here we show that two cytokines, previously shown to be released in response to RSV infection, IL-1β and TNF-α were able to elicit DCP1 phosphorylation in HEp-2 cells (Figure 2C), which could explain why RSV-infected-cell supernatant has an effect. These findings indicate that RSV infection of epithelial cells elicits DCP1 phosphorylation through at least two paths: direct exposure to the virus itself, and through an indirect effect due to cytokines that are released in the course of infection. It is likely a combination of these factors that leads to sustained DCP1 phosphorylation over the infection period.

The pathway responsible for DCP1 phosphorylation, at least during the initial virus-induced stimulus, was found to be ERK1/2. Similarly to other groups, we found that ERK1/2 was activated shortly after exposure of cells to RSV (33) and this activation correlated with DCP1 phosphorylation (Figure 4A). In addition, we found that ERK1/2 chemical inhibitors inhibited RSV-mediated DCP1 phosphorylation (Figure 4C). RSV also activated p38, as reported previously (34–36), but JNK was not activated to a detectable level. Importantly, neither p38 nor JNK inhibitors had a detectable effect on DCP1 phosphorylation (Figure 4C).

Many studies have shown putative roles for DCP1 phosphorylation, including regulating neuronal development (32), mitosis (20), oocyte maturation (37), adipocyte differentiation (26), and P-body distribution (21). A recent study in mice showed that DCP1 phosphorylation increased its interaction with decapping protein DCP2, forming a complex necessary for mRNA decapping (26). DCP1 phosphorylation is also associated with stress-granule formation and translational arrest in response to oxidative stress (32) and antibiotic treatment (21). In addition, a study has shown that overexpression of DCP1 can result in activated PKR, phosphorylated eIF2α, and translational arrest (38). Together, these studies indicate that RSV-induced DCP1 phosphorylation and accumulation could both function to negatively regulate gene expression. The results presented in Figure 5 show that such regulation does occur, but in a gene specific manner. Overexpression of neither wt nor phosphorylation mutants of DCP1 had a consistent detectable effect on RSV protein expression (or tubulin accumulation) (Figure 5B). In contrast, in three independent experiments, RSV-induced IL-8 expression was affected. Over-expression of wt DCP1, in which DCP1 was predominantly present in the hyper-phosphorylated form (Figure 5A), inhibited IL-8 expression compared to either empty vector or GFP control. However, if mutant DCP1 with any of the three described phosphorylation sites mutated to alanine was transfected into cells, tilting the DCP1 population toward the unphosphorylated form, IL-8 expression was partially restored to levels comparable with the empty vector and GFP controls (Figure 5C). RSV infection alone does not induce host-cell translation inhibition and there is no evidence that RSV has evolved mechanisms to allow selective translation of viral mRNAs. Thus, these results suggest that in this experiment, suppression of IL-8 protein secretion was not due to global translational shut-off, but more likely through a specific

regulatory mechanism. IL-8 could be regulated directly by the decapping pathway targeting IL-8 mRNA, but might also be regulated indirectly. For example, DCP1 phosphorylation has been shown to affect NFκB expression, and in turn, expression of NFκB responsive genes (21). Therefore, additional research will be required to define the mechanism by which RSV induced DCP1 phosphorylation affects secretion of IL-8 protein. We focused on IL-8 because previously IL-8 expression had been shown to be affected by DCP1 phosphorylation (33), and because IL-8 is relevant for RSV pathogenesis. We have not investigated the effect of DCP1 on other RSV-induced chemokines and it would be of interest to determine if the effect that we observed extends more widely. It should be noted that the data presented here are in contrast to findings by Rzeczkowski and coworkers (21). They found that compared to a wt DCP1 control, a phosphorylation-deficient DCP1 mutant completely blocked all IL-1-induced gene expression, including IL-8 production. The reason for the discrepancy between the two studies is unclear; however, there are a number of differences between our experiments, with key differences being the inducer (RSV versus IL-1), the kinase pathway involved (ERK1/2 versus JNK), and the magnitude of the IL-8 response (~45,000 pg/ml following 24 h infection with RSV versus ~750 pg/ml following 8 h treatment with IL-1).

In our experiments, there was no detectable change in P-body size or distribution until late stages of RSV infection, suggesting that DCP1 phosphorylation did not affect P-body assembly or integrity (Figure 3). This is consistent with previous findings that DCP1 depletion with small interfering RNAs has no effect on P-body size or number (19). In addition, we found that DCP1 levels were increased at later times of RSV infection (Figure 1), but the reason for this is not known. However, the different phosphorylation-mutant DCP1 proteins were expressed at similar levels compared to wt DCP1 (Figure 5A), indicating that the increase in the level of DCP1 protein was not a consequence of a change in DCP1 stability due to it being phosphorylated, but due to another effect of RSV infection.

RSV is not the only virus to have been shown to have an effect on DCP1. Poliovirus 3C proteinase has been shown to cleave DCP1 and P-body proteins XrnI and Pan3 (39). Cleavage of XrnI and Pan3 could be of benefit to poliovirus by increasing the stability of viral RNAs, but the significance of DCP1 cleavage for poliovirus is less clear. As discussed by the authors of this study, it is possible that disruption of the decapping pathway could have an effect on innate immune responses. In light of the previous findings regarding poliovirus and the results presented here, it is interesting to speculate whether RSV has evolved to mediate DCP1 phosphorylation during infection in order to increase its fitness, or whether DCP1 phosphorylation is important for cellular responses to viral infection. Based on the available evidence, we suggest that DCP1 phosphorylation is an element of the host response. MAP kinases, including ERK1/2, play an important role in regulating the innate immune responses (40) and there are a number of studies indicating that the ERK1/2 pathway is key in promoting the innate immune response to RSV (34, 41, 42). If the ERK1/2 pathway is the only kinase pathway responsible for transducing a signal to stimulate DCP1 phosphorylation during infection, as suggested by the data shown in Figure 4C, it seems unlikely that RSV evolved to stimulate ERK1/2 and DCP1 phosphorylation for its own benefit, especially given that the phosphorylation status of DCP1 had no effect on RSV protein expression (Figure 5B). Rather, it is more likely that ERK1/2-mediated DCP1

phosphorylation is part of an integrated cellular response to the invading virus. Experiments testing the effect of an ERK1/2 inhibitor in RSV infected cells have suggested that the ERK1/2 pathway is important for stimulating the IL-8 response (33). Activation of the innate immune response through MAPK pathways also generally involves induction of negative regulatory loops to limit inflammatory damage (40). Therefore, we propose that RSV-induced, ERK1/2-dependent DCP1 phosphorylation is part of a coordinated cellular response that allows innate immune responses to be modulated.

MATERIALS AND METHODS

Cell lines and antibodies

HEp-2 cells (ATCC) were cultured in Opti-MEM with 2% fetal bovine serum (FBS) (GIBCO-Invitrogen). A549 cells (ATCC) were cultured in F-12K medium supplemented with 10% FBS (GIBCO-Invitrogen). Both cell lines were incubated at 37°C with 5% CO_2. The following antibodies were used in this study: mouse anti-RSV nucleoprotein antibody (Serotec), rabbit anti-DCP1 and goat anti-RSV proteins antibodies (Abcam), goat anti-Xrn1, anti-EDC3, anti-EDC4, anti-TIAR, and anti-TIA-1 antibodies (Santa Cruz), goat anti-G3BP antibodies (BD Biosciences), rabbit anti-p44/42 MAPK (ERK1/2), rabbit anti-phospho-p44/42 MAPK (ERK1/2) (Thr202/Tyr204), rabbit anti-p38 MAPK, anti-phospho-p38 MAPK (Thr180/Tyr182), rabbit anti-SAPK/JNK, rabbit anti-phospho-SAPK/JNK (Thr183/Tyr185), rabbit anti-ERK5, and rabbit anti-phospho-ERK5 (Thr218 / Tyr220) antibodies (Cell Signaling Technology).

RSV stocks

To propagate RSV (strain A2), ~80% confluent HEp-2 cells in 150 cm^2 flasks were infected with RSV at an moi of 0.01 in 10 ml Opti-MEM + 2% FBS. One to four h post infection, media were replaced with 20 ml fresh media. Media was changed every 36–48 hours. Once extensive syncytia formation was observed, cells and supernatant were collected in 50-ml conical tubes and subjected to two rounds of vortexing (10 s) and sonication (30 s) to detached cell-associated virions. The cell suspension was then subjected to centrifugation at 300 × *g* at 4°C for 5 minutes and supernatant was collected, flash frozen, and stored at −80°C. RSV titers were determined by plaque assay as described previously (16). To sucrose purify RSV, fresh virus suspensions were pelleted through 30% sucrose onto a 60% sucrose cushion (sucrose w/v in 10 mM Tris, pH 8.1) by centrifugation at 24,000 × *g* for 1 h at 4 °C. The white band at the 30/60% sucrose interface was collected, diluted 1:10 in OptiMem supplemented with 50 mM HEPES and 100 mM $MgSO_4$, flash frozen, and stored at −80 °C. As a control to ensure that the sucrose that would be present in the purified virus did not have an effect on DCP1 phosphorylation, 60% sucrose was diluted 1:10 in OptiMem solution described above, similarly to the sucrose purified virus, and cells were treated with an equivalent volume of this sucrose solution as the volume of sucrose-purified RSV used for the virus infection. To prepare RSV-free supernatant, virus suspensions were subjected to centrifugation at 24,000 × *g* for 1 h at 4 °C and samples from the supernatant fraction were taken. Titers of infectious virus in unpurified and sucrose-purified RSV and virus-cleared supernatant were determined by plaque assay as described previously (16). UV-inactivated virus was generated by exposing virus in 6-well plates to 200 J/m^2,

approximately 15 cm from light source. UV-inactivation of RSV was confirmed by plaque assay. HEp-2 cells or A549 cells were infected with unpurified, sucrose purified, or treated with UV-inactivated RSV, as described in the figure legends, for 1–2 h at 37 °C. Media was changed and cells were incubated at 37 °C for the times indicated.

Cell harvesting and Western blot analysis

Cells were lysed in RIPA buffer (Boston Bioproducts) with protease inhibitors (Roche) and HALT phosphatase inhibitors (Roche) according to the manufacturer's instructions, unless otherwise specified. Cells were incubated on ice for 10 minutes, after which supernatants were collected in microcentrifuge tubes, vortexed, and subjected to centriguation at 16,000 × *g* for 10 minutes at 4°C. Soluble fractions were collected and added to 2X Laemmli buffer (BioRad) with 0.1 M dithiothreitol. Samples were separated on 10% SDS polyacrylamide gels, transferred to nitrocellulose membranes, blocked with either TBS plus 5% milk or Odyssey blocking buffer (LI-COR) overnight at 4°C, and probed with appropriate antibodies. Membranes were analyzed either by chemiluminescence (Western Lighting Chemiluminescence Reagent, Perkin Elmer), or LI-COR imaging with the LI-COR Odyssey reader. Protein bands were quantified using LI-COR Image Studio software.

Phosphatase Assay

HEp-2 cells were mock infected, treated with 0.5 mM sodium arsenite for 30 minutes immediately prior to harvest, or infected with RSV (moi=5). Cells were lysed in RIPA buffer and centrifuged at 16,000 × *g* for 10 minutes at 4°C. The soluble fraction was collected and then either mock treated or treated with λ-phosphatase (Santa Cruz) according to the manufacturer's instructions before being analyzed by Western blotting, as described above.

Treatment of uninfected cells with cytokines

Monolayers of uninfected HEp-2 cells were treated with 1, 3, or 10 ng / ml of IL-1β or TNF-α (R&D systems), or 10, 30, or 100 U/ml of IFN-α (PBL). One hour post treatment, cells were lysed in RIPA buffer containing protease and phosphatase inhibitors, and DCP1 phosphorylation was assessed using Western blot analysis.

Kinase inhibitor assay

80% confluent HEp-2 cells were mock treated with DMSO or treated with 1 μM 7-oxozeanenol, 1 μM U0126, 20 μM PD98059, 2 μM PD184352, 20 μM PD184352, 20 μM SB203580, or 20 μM SP600125. One hour post treatment, cells were mock infected, infected with sucrose-purified RSV (moi =5), or treated with 0.5 mM sodium arsenite. One hour post infection or 30 minutes following arsenite treatment, cells were harvested and analyzed for DCP1 phosphorylation using Western blot analysis as described above.

Generation and analysis of DCP1 phosphorylation mutants

A myc-DDK-tagged open reading frame DNA clone of human DCP1a (Origene) was subjected to mutagenesis to generate constructs in which S315, S319, T321, or all three residues (Triple) were replaced with alanine using an Agilent Quickchange II site-directed

mutagenesis kit, according to the manufacturer's directions. The sequences of the mutant DDK-DCP1 cassettes were confirmed by DNA sequencing. 80% confluent monolayers of HEp-2 cells in 6-well plates were transfected with 2 μg of empty-vector plasmids or plasmids encoding GFP, wt DDK-DCP1a, or mutant DDK-DCP1a using Lipofectamine 2000 (Invitrogen) according to the manufacturer's instructions. Media were replaced 6 hours post transfection. 24 hours post transfection, cells were infected with RSV (moi =5). At the indicated times post infection, either cell lysates or supernatant were harvested for Western blot or ELISA analysis, respectively.

IL-8 quantification

HEp-2 cells transfected with wt DDK-DCP1a or mutant DDK-DCP1a were infected with RSV at an moi of 5 as described above and incubated for 24 hours. Cell culture supernatants were harvested at 0, 2, 8, and 24 hpi and IL-8 concentrations were determined by ELISA (Biolegend) by comparison to an IL-8 standard curve, according to the manufacturer's instructions.

Immunofluorescence microscopy

HEp-2 cells seeded on coverslips in 12-well plates were either mock infected or infected with wt RSV at moi of 5. At indicated times post infection, cells were fixed with 5% formaldehyde and 2% sucrose in PBS for 30 min, permeabilized with 0.5% Igepal and 10% sucrose in PBS for 20 min at 4 °C, and incubated with a rabbit polyclonal antibody toward cellular DCP1 and a mouse monoclonal antibody toward RSV N protein. Following washing in PBS, cells were incubated with anti-rabbit AlexaFluor 488 and anti-mouse AlexaFluor 633 (Invitrogen), as well as 4′6-diamindino-2-phenylindole (DAPI). Cells were analyzed by fluorescence microscopy and the numbers of DCP1-containing puncta per cell were determined using ImageJ.

Acknowledgments

This work was funded by NIH grant R01AI074903 to R.F. and Boston University School of Medicine. We thank Michael Mawhorter for critical reading of the manuscript and technical assistance.

References

1. Welliver RC. Review of epidemiology and clinical risk factors for severe respiratory syncytial virus (RSV) infection. The Journal of pediatrics. 2003; 143(5 Suppl):S112–7. Epub 2003/11/15. [PubMed: 14615709]
2. Aherne W, Bird T, Court SD, Gardner PS, McQuillin J. Pathological changes in virus infections of the lower respiratory tract in children. Journal of clinical pathology. 1970; 23(1):7–18. Epub 1970/02/01. [PubMed: 4909103]
3. Zhang Y, Luxon BA, Casola A, Garofalo RP, Jamaluddin M, Brasier AR. Expression of respiratory syncytial virus-induced chemokine gene networks in lower airway epithelial cells revealed by cDNA microarrays. Journal of virology. 2001; 75(19):9044–58. Epub 2001/09/05. 10.1128/JVI.75.19.9044-9058.2001 [PubMed: 11533168]
4. Everard ML, Swarbrick A, Wrightham M, McIntyre J, Dunkley C, James PD, Sewell HF, Milner AD. Analysis of cells obtained by bronchial lavage of infants with respiratory syncytial virus infection. Archives of disease in childhood. 1994; 71(5):428–32. Epub 1994/11/01. [PubMed: 7826113]

5. Mastronarde JG, He B, Monick MM, Mukaida N, Matsushima K, Hunninghake GW. Induction of interleukin (IL)-8 gene expression by respiratory syncytial virus involves activation of nuclear factor (NF)-kappa B and NF-IL-6. The Journal of infectious diseases. 1996; 174(2):262–7. Epub 1996/08/01. [PubMed: 8699053]

6. Wang SZ, Xu H, Wraith A, Bowden JJ, Alpers JH, Forsyth KD. Neutrophils induce damage to respiratory epithelial cells infected with respiratory syncytial virus. The European respiratory journal. 1998; 12(3):612–8. Epub 1998/10/08. [PubMed: 9762789]

7. Krzyzaniak MA, Zumstein MT, Gerez JA, Picotti P, Helenius A. Host cell entry of respiratory syncytial virus involves macropinocytosis followed by proteolytic activation of the F protein. PLoS pathogens. 2013; 9(4):e1003309. Epub 2013/04/18. 10.1371/journal.ppat.1003309 [PubMed: 23593008]

8. Collins PL, Fearns R, Graham BS. Respiratory syncytial virus: virology, reverse genetics, and pathogenesis of disease. Current topics in microbiology and immunology. 2013; 372:3–38. Epub 2013/12/24. 10.1007/978-3-642-38919-1_1 [PubMed: 24362682]

9. Fricke J, Koo LY, Brown CR, Collins PL. p38 and OGT sequestration into viral inclusion bodies in cells infected with human respiratory syncytial virus suppresses MK2 activities and stress granule assembly. Journal of virology. 2013; 87(3):1333–47. Epub 2012/11/16. 10.1128/JVI.02263-12 [PubMed: 23152511]

10. Garcia J, Garcia-Barreno B, Vivo A, Melero JA. Cytoplasmic inclusions of respiratory syncytial virus-infected cells: formation of inclusion bodies in transfected cells that coexpress the nucleoprotein, the phosphoprotein, and the 22K protein. Virology. 1993; 195(1):243–7. Epub 1993/07/01. 10.1006/viro.1993.1366 [PubMed: 8317099]

11. Lloyd RE. How do viruses interact with stress-associated RNA granules? PLoS pathogens. 2012; 8(6):e1002741. Epub 2012/07/05. 10.1371/journal.ppat.1002741 [PubMed: 22761570]

12. Lloyd RE. Regulation of stress granules and P-bodies during RNA virus infection. Wiley interdisciplinary reviews. RNA. 2013; 4(3):317–31. Epub 2013/04/05. 10.1002/wrna.1162 [PubMed: 23554219]

13. Pattnaik AK, Dinh PX. Manipulation of cellular processing bodies and their constituents by viruses. DNA and cell biology. 2013; 32(6):286–91. Epub 2013/04/27. 10.1089/dna.2013.2054 [PubMed: 23617258]

14. Reineke LC, Lloyd RE. Diversion of stress granules and P-bodies during viral infection. Virology. 2013; 436(2):255–67. Epub 2013/01/08. 10.1016/j.virol.2012.11.017 [PubMed: 23290869]

15. Anderson P. Post-transcriptional control of cytokine production. Nature immunology. 2008; 9(4): 353–9. Epub 2008/03/20. 10.1038/ni1584 [PubMed: 18349815]

16. Hanley LL, McGivern DR, Teng MN, Djang R, Collins PL, Fearns R. Roles of the respiratory syncytial virus trailer region: effects of mutations on genome production and stress granule formation. Virology. 2010; 406(2):241–52. Epub 2010/08/13. 10.1016/j.virol.2010.07.006 [PubMed: 20701943]

17. Lindquist ME, Lifland AW, Utley TJ, Santangelo PJ, Crowe JE Jr. Respiratory syncytial virus induces host RNA stress granules to facilitate viral replication. Journal of virology. 2010; 84(23): 12274–84. Epub 2010/09/17. 10.1128/JVI.00260-10 [PubMed: 20844027]

18. Groskreutz DJ, Babor EC, Monick MM, Varga SM, Hunninghake GW. Respiratory syncytial virus limits alpha subunit of eukaryotic translation initiation factor 2 (eIF2alpha) phosphorylation to maintain translation and viral replication. The Journal of biological chemistry. 2010; 285(31): 24023–31. Epub 2010/06/04. 10.1074/jbc.M109.077321 [PubMed: 20519500]

19. Eulalio A, Behm-Ansmant I, Izaurralde E. P bodies: at the crossroads of post-transcriptional pathways. Nature reviews Molecular cell biology. 2007; 8(1):9–22. Epub 2006/12/22. 10.1038/nrm2080

20. Aizer A, Kafri P, Kalo A, Shav-Tal Y. The P body protein Dcp1a is hyper-phosphorylated during mitosis. PloS one. 2013; 8(1):e49783. Epub 2013/01/10. 10.1371/journal.pone.0049783 [PubMed: 23300942]

21. Rzeczkowski K, Beuerlein K, Muller H, Dittrich-Breiholz O, Schneider H, Kettner-Buhrow D, Holtmann H, Kracht M. c-Jun N-terminal kinase phosphorylates DCP1a to control formation of P

bodies. The Journal of cell biology. 2011; 194(4):581–96. Epub 2011/08/24. 10.1083/jcb.201006089 [PubMed: 21859862]

22. Parker R, Song H. The enzymes and control of eukaryotic mRNA turnover. Nature structural & molecular biology. 2004; 11(2):121–7. Epub 2004/01/30. 10.1038/nsmb724
23. Patel JA, Kunimoto M, Sim TC, Garofalo R, Eliott T, Baron S, Ruuskanen O, Chonmaitree T, Ogra PL, Schmalstieg F. Interleukin-1 alpha mediates the enhanced expression of intercellular adhesion molecule-1 in pulmonary epithelial cells infected with respiratory syncytial virus. American journal of respiratory cell and molecular biology. 1995; 13(5):602–9. Epub 1995/11/01. 10.1165/ajrcmb.13.5.7576697 [PubMed: 7576697]
24. Hornung V, Schlender J, Guenthner-Biller M, Rothenfusser S, Endres S, Conzelmann KK, Hartmann G. Replication-dependent potent IFN-alpha induction in human plasmacytoid dendritic cells by a single-stranded RNA virus. Journal of immunology. 2004; 173(10):5935–43. Epub 2004/11/06.
25. Jewell NA, Vaghefi N, Mertz SE, Akter P, Peebles RS Jr, Bakaletz LO, Durbin RK, Flano E, Durbin JE. Differential type I interferon induction by respiratory syncytial virus and influenza a virus in vivo. Journal of virology. 2007; 81(18):9790–800. Epub 2007/07/13. 10.1128/JVI.00530-07 [PubMed: 17626092]
26. Chiang PY, Shen YF, Su YL, Kao CH, Lin NY, Hsu PH, Tsai MD, Wang SC, Chang GD, Lee SC, Chang CJ. Phosphorylation of mRNA decapping protein Dcp1a by the ERK signaling pathway during early differentiation of 3T3-L1 preadipocytes. PloS one. 2013; 8(4):e61697. Epub 2013/05/03. 10.1371/journal.pone.0061697 [PubMed: 23637887]
27. Lee J, Mira-Arbibe L, Ulevitch RJ. TAK1 regulates multiple protein kinase cascades activated by bacterial lipopolysaccharide. Journal of leukocyte biology. 2000; 68(6):909–15. Epub 2000/12/29. [PubMed: 11129660]
28. Ear T, Fortin CF, Simard FA, McDonald PP. Constitutive association of TGF-beta-activated kinase 1 with the IkappaB kinase complex in the nucleus and cytoplasm of human neutrophils and its impact on downstream processes. J Immunol. 184(7):3897–906. Epub 2010/03/05. [pii]. 10.4049/jimmunol.0902958 [PubMed: 20200282]
29. Sato S, Sanjo H, Takeda K, Ninomiya-Tsuji J, Yamamoto M, Kawai T, Matsumoto K, Takeuchi O, Akira S. Essential function for the kinase TAK1 in innate and adaptive immune responses. Nature immunology. 2005; 6(11):1087–95. Epub 2005/09/28. 10.1038/ni1255 [PubMed: 16186825]
30. Davies SP, Reddy H, Caivano M, Cohen P. Specificity and mechanism of action of some commonly used protein kinase inhibitors. The Biochemical journal. 2000; 351(Pt 1):95–105. Epub 2000/09/22. [PubMed: 10998351]
31. Tanemura S, Momose H, Shimizu N, Kitagawa D, Seo J, Yamasaki T, Nakagawa K, Kajiho H, Penninger JM, Katada T, Nishina H. Blockage by SP600125 of Fcepsilon receptor-induced degranulation and cytokine gene expression in mast cells is mediated through inhibition of phosphatidylinositol 3-kinase signalling pathway. Journal of biochemistry. 2009; 145(3):345–54. Epub 2008/12/25. 10.1093/jb/mvn172 [PubMed: 19106158]
32. Blumenthal J, Behar L, Elliott E, Ginzburg I. Dcp1a phosphorylation along neuronal development and stress. FEBS letters. 2009; 583(1):197–201. Epub 2008/12/17. 10.1016/j.febslet.2008.12.002 [PubMed: 19084008]
33. Chen W, Monick MM, Carter AB, Hunninghake GW. Activation of ERK2 by respiratory syncytial virus in A549 cells is linked to the production of interleukin 8. Experimental lung research. 2000; 26(1):13–26. Epub 2000/02/08. [PubMed: 10660833]
34. Pazdrak K, Olszewska-Pazdrak B, Liu T, Takizawa R, Brasier AR, Garofalo RP, Casola A. MAPK activation is involved in posttranscriptional regulation of RSV-induced RANTES gene expression. American journal of physiology Lung cellular and molecular physiology. 2002; 283(2):L364–72. Epub 2002/07/13. 10.1152/ajplung.00331.2001 [PubMed: 12114198]
35. Singh D, McCann KL, Imani F. MAPK and heat shock protein 27 activation are associated with respiratory syncytial virus induction of human bronchial epithelial monolayer disruption. American journal of physiology Lung cellular and molecular physiology. 2007; 293(2):L436–45. Epub 2007/06/15. 10.1152/ajplung.00097.2007 [PubMed: 17557802]
36. Tu HY, Chen X, Li J. Signal transduction in respiratory syncytial virus infection-induced thymic stromal lymphopoietin expression in human epithelial cells. Nan fang yi ke da xue xue bao =

Journal of Southern Medical University. 2007; 27(10):1581–3. Epub 2007/10/26. [PubMed: 17959543]

37. Ma J, Flemr M, Strnad H, Svoboda P, Schultz RM. Maternally recruited DCP1A and DCP2 contribute to messenger RNA degradation during oocyte maturation and genome activation in mouse. Biol Reprod. 88(1):11. Epub 2012/11/09. [pii]. 10.1095/biolreprod.112.105312 [PubMed: 23136299]
38. Dougherty JD, Reineke LC, Lloyd RE. mRNA decapping enzyme 1a (Dcp1a)-induced translational arrest through protein kinase R (PKR) activation requires the N-terminal enabled vasodilator-stimulated protein homology 1 (EVH1) domain. The Journal of biological chemistry. 2014; 289(7):3936–49. Epub 2014/01/03. 10.1074/jbc.M113.518191 [PubMed: 24382890]
39. Dougherty JD, White JP, Lloyd RE. Poliovirus-mediated disruption of cytoplasmic processing bodies. Journal of virology. 2011; 85(1):64–75. Epub 2010/10/22. 10.1128/JVI.01657-10 [PubMed: 20962086]
40. Arthur JS, Ley SC. Mitogen-activated protein kinases in innate immunity. Nature reviews Immunology. 2013; 13(9):679–92. Epub 2013/08/21. 10.1038/nri3495
41. Kato M, Ishioka T, Kita H, Kozawa K, Hayashi Y, Kimura H. Eosinophil granular proteins damage bronchial epithelial cells infected with respiratory syncytial virus. International archives of allergy and immunology. 2012; 158 (Suppl 1):11–8. Epub 2012/06/01. 10.1159/000337752 [PubMed: 22627361]
42. Monick MM, Cameron K, Staber J, Powers LS, Yarovinsky TO, Koland JG, Hunninghake GW. Activation of the epidermal growth factor receptor by respiratory syncytial virus results in increased inflammation and delayed apoptosis. The Journal of biological chemistry. 2005; 280(3): 2147–58. Epub 2004/11/16. 10.1074/jbc.M408745200 [PubMed: 15542601]

HIGHLIGHTS

- Exposure of epithelial cells to RSV resulted in rapid phosphorylation of DCP1.
- DCP1 phosphorylation could be induced by purified RSV.
- DCP1 phosphorylation was also induced by cytokines released during RSV infection.
- RSV-induced phosphorylation of DCP1 required the ER1/2 pathway.
- DCP1 phosphorylation modulated RSV-induced IL-8 production.

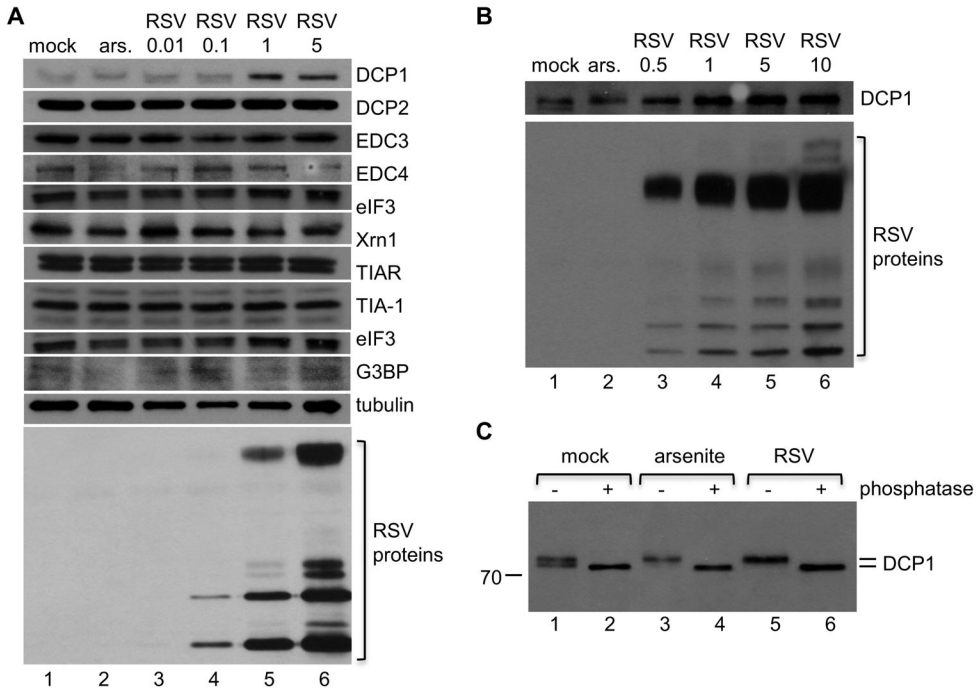

Figure 1. Exposure of cells to RSV results in phosphorylation of DCP1

(A and B) HEp-2 (A) or A549 cells (B) were mock infected, treated with 0.5 mM sodium arsenite for 30 minutes (ars.), or infected with RSV at an moi of 0.01 to 10 pfu/cell, as indicated. 18 hour post infection, cells were lysed and soluble fractions of samples were assessed by Western blot analysis using antibodies toward the indicated proteins. (C) HEp-2 cells were mock infected, treated with sodium arsenite, or infected with RSV (moi of 5) for one hour. Samples were lysed and soluble fractions were either mock treated or treated with λ phosphatase. Samples were examined by Western blot analysis using an antibody toward DCP1a. Data are representative of at least three independent experiments.

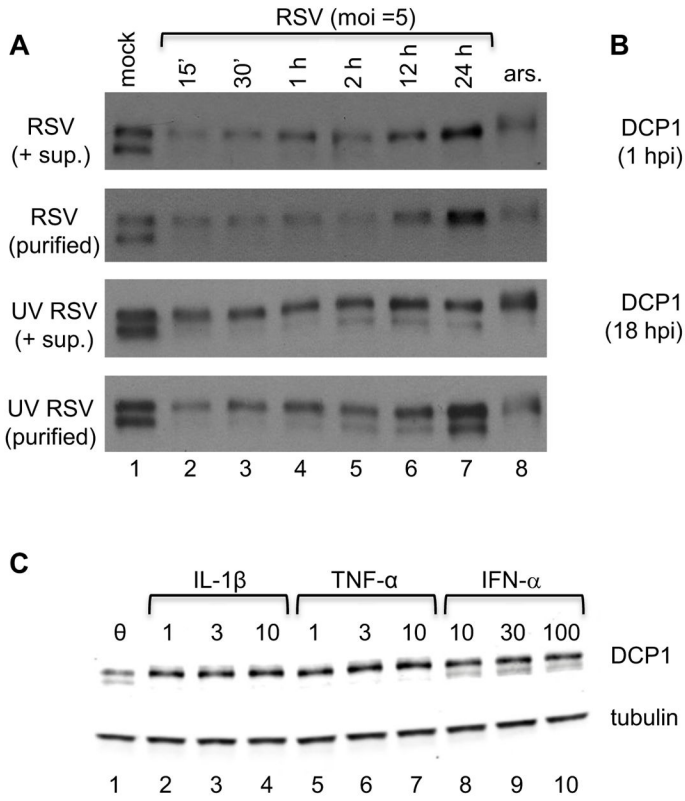

Figure 2. DCP1 phosphorylation occurs rapidly following exposure of cells to RSV

(A) HEp-2 cells were mock infected, infected with RSV or UV-inactivated RSV (containing cell supernatant), or with sucrose-purified RSV, or UV-inactivated, sucrose-purified RSV, or treated with 0.5 mM sodium arsenite (ars.). Samples were lysed at the indicated times post infection and soluble fractions were analyzed by Western blotting using an antibody toward DCP1a. (B) HEp-2 cells were mock infected, treated with supernatant (sup.) from RSV-infected cells that was subjected to centrifugation at 24,000 × *g* at 4 °C for 1 hour (to remove virus), or infected with sucrose-purified RSV (moi of 5). One or eighteen hours post treatment/infection (upper and lower panels, respectively), cells were lysed and examined using Western blot analysis with an antibody towards DCP1. (C) Treatment of uninfected HEp-2 cells with cytokines. Uninfected HEp-2 cells were treated with 1, 3, or 10 ng / ml of IL-1β or TNF-α, or 10, 30, or 100 U/ml of IFN- α for 1 hour and then lysed and examined using Western blot analysis with an antibody towards DCP1a. In panels A and B, data are representative of at least three independent experiments; panel C is representative of two independent experiments.

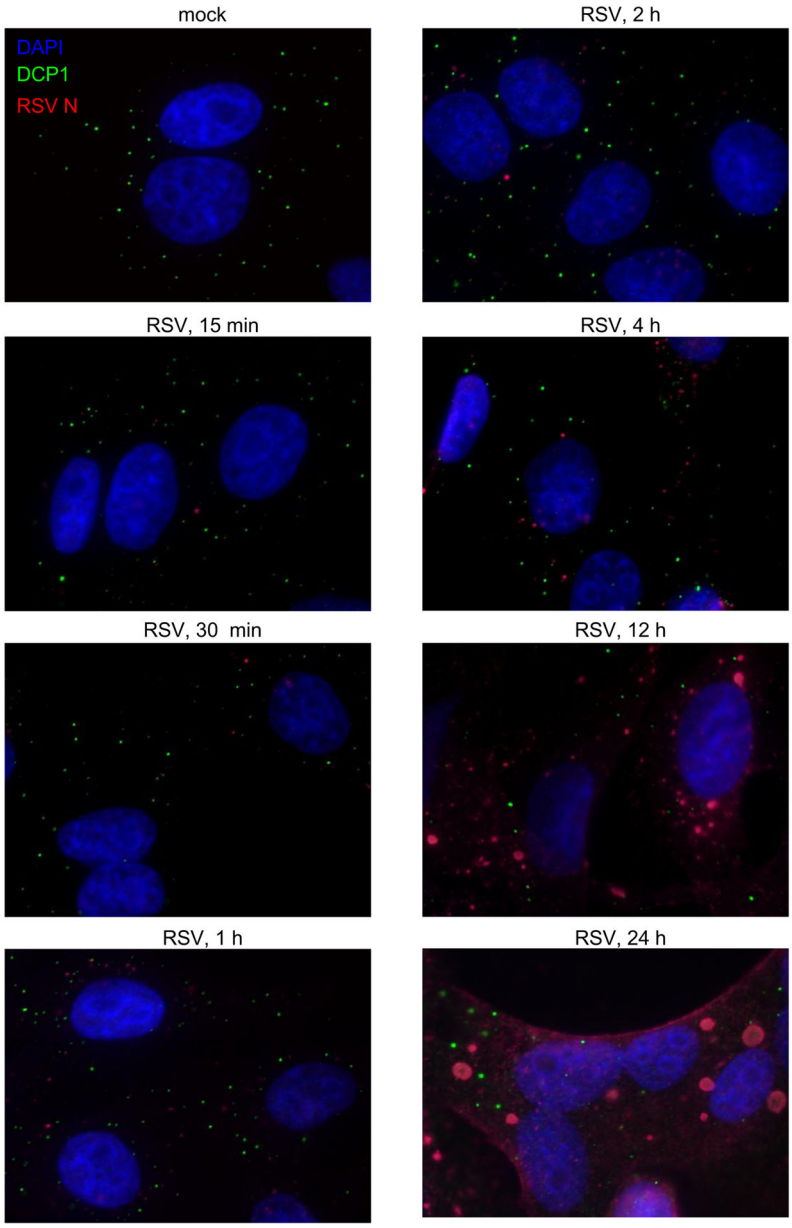

Figure 3. Effect of RSV infection on P-body distribution

HEp-2 cells were mock infected or infected with RSV at an moi of 5. Cells were fixed at the indicated time post infection and analyzed using immunofluorescence with antibodies toward DCP1 (green) and RSV N protein (red). Cells were also stained with DAPI to visualize nuclei. Results are representative of two independent experiments.

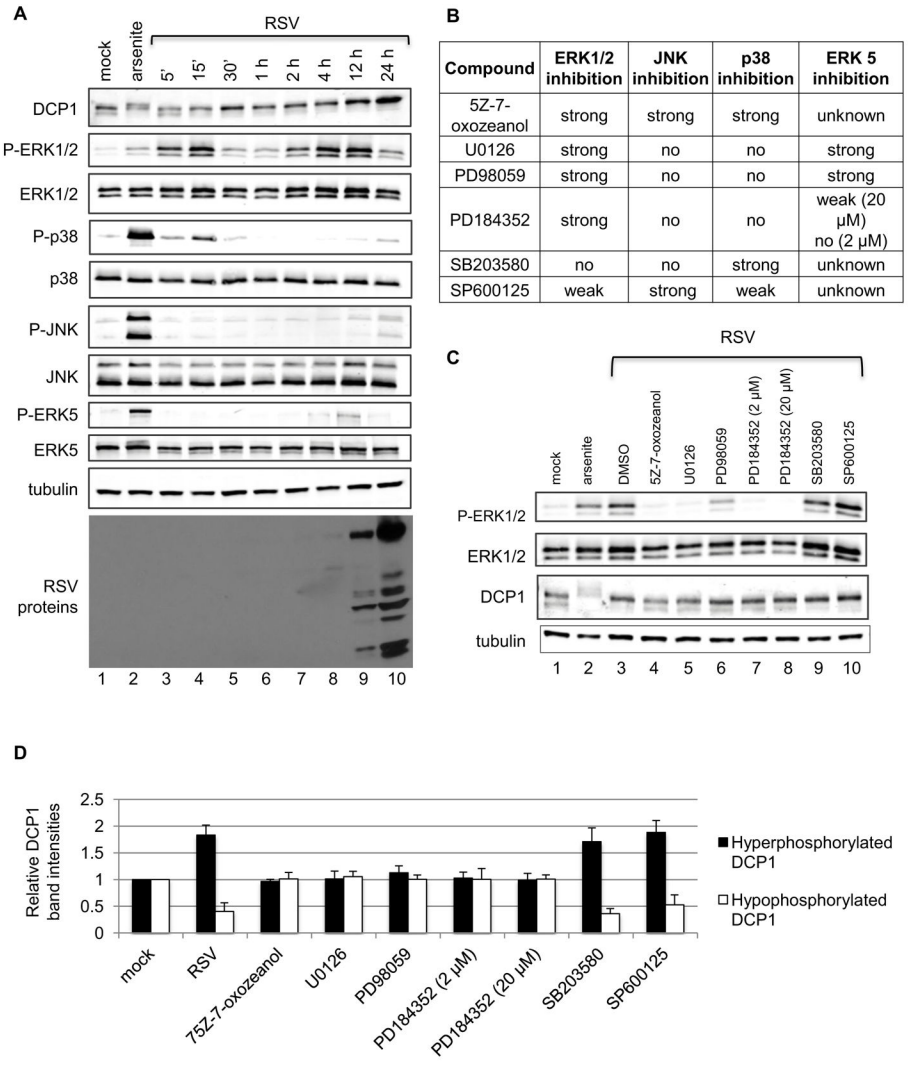

Compound	ERK1/2 inhibition	JNK inhibition	p38 inhibition	ERK 5 inhibition
5Z-7-oxozeanol	strong	strong	strong	unknown
U0126	strong	no	no	strong
PD98059	strong	no	no	strong
PD184352	strong	no	no	weak (20 μM) no (2 μM)
SB203580	no	no	strong	unknown
SP600125	weak	strong	weak	unknown

Figure 4. RSV-mediated DCP1 phosphorylation is ERK1/2 dependent

(A) HEp-2 cells were mock infected or infected with sucrose-purified RSV (moi of 5). Cell lysates were collected at indicated times post infection and analyzed by Western blotting with antibodies against phosphorylated (P-) and total populations of the indicated proteins. Lane 2 is a control in which cells were treated with arsenite for 30 minutes prior to harvest. (B) MAPK inhibitors used and their relative activities against the different MAP kinases. (C) HEp-2 cells were mock treated with DMSO or treated with indicated inhibitors for one hour. The cells were then mock infected or infected with sucrose purified RSV (moi of 5) for one hour in the presence of inhibitor and harvested. Samples were analyzed by Western blotting with antibodies against the indicated proteins. (D) Hyperphosphorylated (upper band) and hypophosphorylated (lower band) DCP1 from kinase-inhibitor samples were quantified using LI-COR Odyssey software, and are displayed as mean fold difference + SEM compared to those of mock-infected, mock-treated samples. All data are representative of at least three independent experiments.

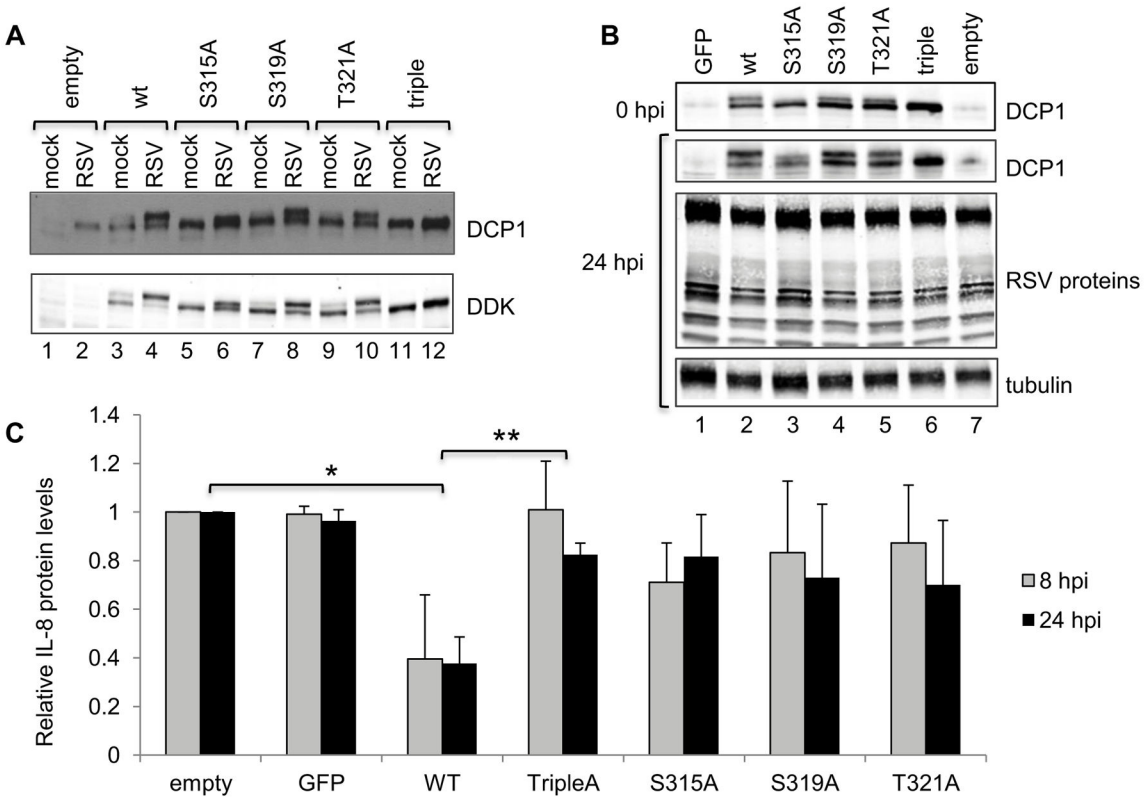

Figure 5. RSV-mediated DCP1 phosphorylation affects RSV induced IL-8 production

(A) Identification of DCP1 phosphorylation sites during RSV infection. HEp-2 cells were transfected with empty vector or constructs expressing wt DDK-tagged DCP1, or DDK-DCP1 in which residues S315, S319, and/or T321 were mutated to alanine. At 24 h post transfection, cells were infected with RSV (moi of 5), and 24 h post infection cells were harvested. Cell lysates were analyzed by Western blotting with antibodies against DCP1 or DDK, as indicated. (B) DCP1 does not affect RSV protein expression over a single cycle. HEp-2 cells in duplicate were transiently transfected with constructs expressing wt DCP1, or DCP1 in which S315, S319, and/or T321 were mutated to alanine residues. Cells were transfected with either empty vector, or vector expressing GFP, as negative controls. At 24 h post transfection, cells were infected with RSV (moi = 5). At 0 and 24 hpi cells were harvested and analyzed by Western blotting with indicated antibodies. (C) DCP1 phosphorylation inhibits IL-8 protein expression. Concentrations of secreted IL-8 in the cell supernatants at 8 and 24 h post infection from the experiment shown in panel B were determined by ELISA. In each experiment, the IL-8 values were normalized to the values obtained with empty vector at 8 and 24 hpi. The bar chart shows the mean and standard deviation of three (GFP, S315A, S319A and T321A) or four (empty, wt and Triple) independent experiments. Statistical significance was determined using Student's paired T-tests on IL-8 concentration values (* p=0.0386, **p=0.0405).